Original Research

Combining Spatial and Temporal Information to Explore Function-Guide Action of Acupuncture Using fMRI

Peng Liu, PhD,[1] Wei Qin, PhD,[2] Yi Zhang, PhD,[2] Jie Tian, PhD,[2,3] Lijun Bai, PhD,[2] Guangyu Zhou, MS,[2] Jixin Liu, PhD,[2] Peng Chen, MD,[4] Jianping Dai, MD,[5] Karen M. von Deneen, MD,[6] and Yijun Liu, PhD[6]*

Purpose: To investigate the brain response patterns of modulation of GB37 (Guangming) and KI8 (Jiaoxin).

Materials and Methods: An experiment using nonrepeated event-related fMRI design was carried out on 28 subjects with electroacupuncture stimulation (EAS) at GB37 or KI8 on the left leg. The discrete cosine transform and functional connectivity methods were adopted to detect the differences related with these two acupoints before and after the EAS.

Results: Spatial patterns were distinct for EAS at the two acupoints, and the overlapping brain regions were mainly located in the posterior cingulate cortex (PCC) and precuneus (pC). Two opposite patterns of modulation in the default mode network were detected from the temporal patterns with the overlapping PCC/pC as the region of interest. Furthermore, the specific responses of sustained effects at these acupoints were also identified.

Conclusion: Spatial and temporal patterns of the sustained effect modulation of GB37 and KI8 were distinct. We suggest these findings may attribute to the functional specificity of a certain acupoint. Moreover, our current results reflect a significant methodological contribution to future acupuncture studies.

Key Words: spatial and temporal patterns; functional brain networks; fMRI; acupuncture
J. Magn. Reson. Imaging 2009;30:000–000.

[1]School of Sino-Dutch Biomedical and Information Engineering, Northeastern University, Shenyang, Liaoning, China.

[2]Life Science Research Center, School of Electronic Engineering, Xidian University, Xi'an, Shaanxi, China.

[3]Institute of Automation, Chinese Academy of Sciences, Beijing, China.

[4]Beijing Traditional Chinese Medicine Hospital, Capital Medical University, Beijing, China.

[5]Department of Radiology, Beijing Tiantan Hospital, Capital Medical University, Beijing, China.

[6]Department of Psychiatry and Neuroscience, McKnight Brain Institute, University of Florida, Gainesville, Florida.

Contract grant sponsor: Project for the National Key Basic Research and Development Program (973); Contract grant number: 2006CB705700; Contract grant sponsor: Changjiang Scholars and Innovative Research Team in University (PCSIRT); Contract grant number: IRT0645; Contract grant sponsor: Chair Professors of Cheung Kong Scholars Program; Contract grant sponsor: CAS Hundred Talents Program; Contract grant sponsor: CAS Scientific Research Equipment Develop Program; Contract grant number: YZ0642; Contract grant number: YZ200766; Contract grant sponsor: 863 Program; Contract grant number: 2008AA01Z411; Contract grant sponsor: the Joint Research Fund for Overseas Chinese Young Scholars; Contract grant number: 30528027; Contract grant sponsor: the National Natural Science Foundation of China; Contract grant number: 30672690; Contract grant number: 30600151; Contract grant number: 30873462; Contract grant number: 30870685; Contract grant number: 60532050; Contract grant number: 60621001; Contract grant number: 90209008; Contract grant sponsor: Beijing Natural Science Fund; Contract grant number: 4071003.

*Address reprint requests to: J.T., Medical Image Processing Group, Key Laboratory of Complex Systems and Intelligence Science, Institute of Automation Chinese Academy of Science, Graduate School of the Chinese Academy of Science, P.O. Box 2728, Beijing, 100190, China. E-mail: tian@ieee.org

Received December 19, 2008; Accepted April 8, 2009.

DOI 10.1002/jmri.21805
Published online in Wiley InterScience (www.interscience.wiley.com).

ACUPUNCTURE IS ONE of the oldest and most important therapeutic modalities in Traditional Chinese Medicine (TCM). In the past few decades, acupuncture has been selected as a complementary therapy in the Western world (1–3), and a variety of symptoms can be treated by acupuncture in clinical application (4). However, the mechanism underlying the acupuncture has not been clarified to date. With the development of noninvasive fMRI functional brain imaging techniques, this has provided us with more direct information about the neural basis of the acupuncture.

In acupuncture studies, acupoint specificity is well-discussed topic. It was indicated that the visual cortex is activated by laser acupuncture stimulation at the vision-related acupoints (5,6). Li et al detected that stimulation of the vision-implicated acupoints can induce the activations of the vision-related cortex (7). Acupuncture stimulus at the auditory-related acupoint K3 (Taixi) induced activation in the auditory cortex (8). Furthermore, it has been reported that PC6 (Neiguan) is verified to be effective for nausea (9). Daniel et al detected that acupuncture at HN3 (Yintang), NH8 (Yingxiang), and ST36 is effective in the treatment of child-

AQ: 1 hood persistent allergic rhinitis (10). ST36 (Zusanli) and SP6 (Sanyinjiao) are valid for regulating visceral-related disorders (11). Patients with lateral epicondylitis (tennis elbow) can be treated by the acupoints GB34 (Yanglingquan) and ST36 (12). Evidence that the acupoint specificity may exist is supported by these studies. However, several other studies did not attain the same results as described above, especially regarding the specificity of vision-related acupoints. One study from Gareus et al indicated that the significant BOLD signal changes were not detected in the visual cortex induced by acupuncture at GB37 (13). Kong et al indicated that the electroacupuncture stimulation (EAS) manipulation may not induce any significant differences in the occipital cortex among UB60 (Kunlun), GB37, and an adjacent nonacupoint (14). Recently, Cho et al retracted their early research in the *PNAS* article, and they agreed that the specificity of the acupoints does not exist (15). Therefore, it is still not resolved whether or not acupoint specificity is valid.

Previous acupuncture studies investigated the topography of brain activity with experimental tasks based on multiple block designs or single block designs, using fMRI (14,16–20). However, the ON–OFF design should fulfill the assumption that the brain state ends quickly when the ON condition stimulation is over. For example, checkboard visual experiments meet this requirement. Recently, Zhang et al have found the time variability of acupuncture during the multiple block design, meaning that certain effects of acupuncture remained long after stimulation, and the brain state did not return back to the baseline in the OFF-state (21). If block paradigms are used to investigate the acupuncture, the influence of the time variability of acupuncture may influence the estimated results, which has unfortunately been ignored in the majority of acupuncture studies. On the other hand, the acupuncture effects can sustain for several minutes or several hours even after acupuncture stimulation based on the TCM theory and clinical reports. Price et al demonstrated that the analgesic effects of acupuncture actually peak long after acupuncture stimulation (22). Dhond et al reported that the sustained effects of acupuncture can alter the DMN and the sensorimotor network (SMN) after stimulation at left PC6 (Neiguan) (23). Moreover, Qin et al reported that the brain networks related with amygdala are modulated by sustained acupuncture effects (24). Thus, it is seems that the sustained effects are important aspects for acupuncture studies.

In the current study, we investigated the spatial and temporal patterns of brain responses modulated by the sustained effects of vision-related and nonvision-related acupoints, adopting discrete cosine transform (DCT) and functional connectivity methods. DCT is an effective method used to detect the spatial patterns of any signal changes during specific band frequencies (25). Functional connectivity describes the temporal synchrony or correlation of the blood oxygen level-dependent (BOLD) fMRI signal from two or more anatomically separate brain regions (26). We hypothesized that the spatial and temporal patterns of brain responses modulated by the sustained effects of acupuncture were distinct, which might attribute to the function of a certain acupoint.

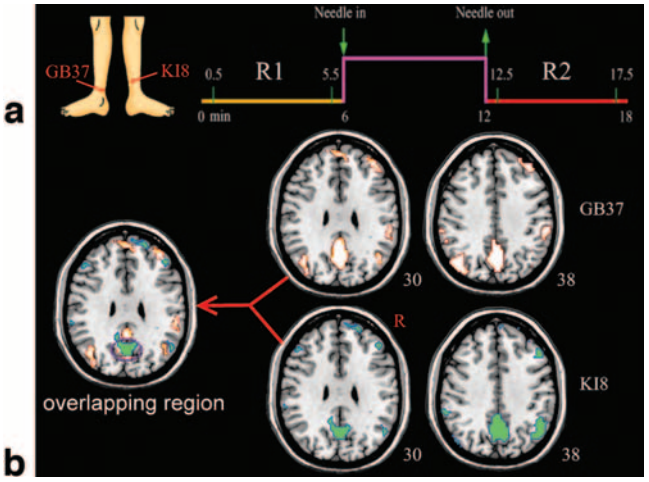

COLOR

Figure 1. a: Experimental paradigm. GB37 and KI8 were located on the left leg. The arrows indicated the time points of needle insertion and withdrawal. The epoch of acupuncture manipulation lasted for 6 min as shown by the pink line. **b:** Results from the conjunction analysis based on the DCT group results of the two acupoints. The overlapping brain regions are located in the PCC/pC enclosed by the purple circle.

MATERIALS AND METHODS

Subjects and Experimental Paradigm

Twenty-eight healthy, right-handed Chinese students (ages, 23.5 ± 2.4 years; mean ± SD) participated in this study. All subjects were all acupuncture naïve and had no history of neurological or psychiatric disorders. Furthermore, all subjects had refrained from alcohol or drug consumption at least 48 h before the experiment. Each subject was given informed consent approved by a local review board for human studies.

All of the 28 subjects were randomized into two groups and variances across subjects were counterbalanced across groups. A nonrepeated event-related (NRER) fMRI design (24) was applied in the current study (Fig. 1a). Before scanning each subject was intro- F1
duced to the principles of acupuncture and fMRI to reduce anxiety. After a 6-min resting scan, one group received treatment by means of a pure stainless steel disposable needle (0.18 mm in diameter and 40 mm in length), which was inserted at GB37, located on the lateral side of the left leg, 5 cm superior to the promi- AQ: 2
nence of the lateral malleolus. The depth of needle ranged from 1 cm to 1.5 cm. And EAS was operated by a professional acupuncturist on each subject for 6 min with 2 Hz pulses and 2–3 mA. The needle was then removed and each subject underwent another 6-min resting scan. The entire scanning run lasted 18 min. In the other group, each subject received the similar treatment mentioned above, but the needle was inserted at KI8, located on posterior to the medial border of the tibia on the left leg. Additionally, two electrodes were separately attached to the acupuncture needle and to a shallowly inserted point 1 cm nearby (the nonacupoint

on GB or KI meridian). The stimulation was delivered with a modified current-constant HANS (Han's Acupoint Nerve Stimulator) LH202 (Neuroscience Research Center, Peking University, Beijing, China).

During the scanning procedure, each subject was instructed to remain still and the head was immobilized with a foam pillow; his/her eyes were also covered with a blindfold and ears were plugged with earplugs. All subjects were asked to remain relaxed and not to think about anything. Finally, the acupuncturist asked each subject whether he/she had slept during scanning. If not, he/she was required to complete the psychophysical response reports.

Psychophysical Data Sets

The participants were asked about the sensations they felt any of the following: aching, soreness, numbness, fullness, sharp or dull pain, pressure, heaviness, warmth, coolness, tingling, itching, and any other sensations. The intensity of each sensation was measured on a scale of 0 to 10 (0 = no sensation, 1–3 = mild, 4–6 = moderate, 7–8 = strong, 9 = severe and 10 = unbearable sensation), as determined by Hui et al (18,27).

MR Imaging

The fMRI experiment was performed using a 3.0 Tesla (T) Signa (GE) MR with a standard head coil. Functional images were acquired with a single-shot gradient-recalled echo planar imaging sequence (TR/TE: 2000 ms/30 ms, field of view (FOV): 240 mm × 240 mm, matrix size: 64 × 64, flip angle: 90°, in-plane resolution: 3.75 mm × 3.75 mm, slice thickness: 5 mm thick with no gaps, 32 sagittal slices). A set of T1-weighted high-resolution structural images was also collected (TR/TE: 5.7 ms/2.2 ms, FOV: 256 mm × 256 mm, matrix size: 256 × 256, flip angle: 12°, in-plane resolution: 1 mm × 1 mm, slice thickness: 1 mm with no gaps).

Image Reprocessing

The first five time points were discarded to avoid the instability of the initial MRI signal. The fMRI runs were intensity scaled to yield a whole brain mode value of 1000 (28). Data sets were preprocessed using SPM5 (www.fil.ion.ucl.ac.uk/spm). Images were realigned to the first image. If translation and rotation were more than 1 mm off in any direction or more than 1 degree from the normal setting, the images were excluded. The images were then normalized to Montreal Neurological Institute template and re-sampled to 3 mm × 3 mm × 3 mm. R1 contained the images from 0.5 min to 5.5 min and the images from 12.5 to 17.5 min were named as R2.

Discrete Cosine Transform Analysis

R2 was smoothed with a 12-mm full width at half maximum (FWHM) Gaussian kernel for the DCT analysis. The DCT analysis was followed by steps depicted in Fransson's study (25). The discrete cosine bias set contained 60 regressors spanning the frequency of 0–0.1Hz. Statistical parametrical maps were constructed by computing F-contrasts, which compared the effect of signal fluctuations in the range of 0.01–0.1Hz. Statistical parametrical maps were created under the threshold $P < 0.005$ (corrected for multiple comparisons) at the first level.

The final overlapping mask was created by multiplying the binary values of the individual mask in each group. Finally, the conjunction analysis of two group masks was applied to detect inter-group similarities of spatial patterns, which was adopted as the ROI for the functional connectivity analysis.

Functional Connectivity Analysis

We applied the ROI for further functional connectivity analysis. First, R1 and R2 were processed with a band-pass-filter of 0.01–0.1 Hz. The data sets were then spatially smoothed with 6 mm FWHM Gaussian kernel. Second, linear regressions were used to remove several spurious variances along with their temporal derivatives: the six head motion parameters, the signals from a region centered in the white matter, and a region centered in the cerebrospinal fluid. Third, correlation maps were created by computing the correlation coefficients between the BOLD time course from the seed region and the BOLD time course from all of the other brain voxels. Finally, correlation coefficients were converted to an approximately normal distribution using Fisher's z-transformation. At the second-level analysis, a two sample t-test was applied to evaluate the baseline scan of the two acupoint groups before EAS. A paired t-test was then used to compare the brain networks before and after EAS. Finally, the test for differences of brain networks between the two groups was evaluated using a two-sample t-test during the poststimulation periods. All contrasts had a threshold at $P < 0.005$ (uncorrected) and a cluster size >3 voxels.

RESULTS

Psychophysical Data Analysis Results

Fullness and numbness were primary *Deqi* sensations reported by most subjects. The frequency of fullness was 50.00% among the subjects at GB37 and 64.19% at KI8 and the frequency of numbness was 71.43% at GB37 and 64.29% at KI8. The intensity of sensation was expressed as follows: the average fullness rating was 4.27 (SD = 2.93) at GB37 and 2.86 (SD = 3.35) at KI8 (P =0.17). The average numbness rating was 2.27 (SD = 3.20) at GB37 and 2.54 (SD = 2.34) at KI8 (P =0.09). The results were also similar when comparing the sharp pain scores between the two points (P = 0.30). All of these did not reach statistical significance for *Deqi* or sharp pain scores. Therefore, the subjective reports from the subjects indicated that the levels of *Deqi* sensations and pain sensations were not significantly different between GB37 and KI8 (two sample t-test, $P < 0.05$).

Discrete Cosine Transform Results

Brain maps of the low-frequency BOLD signal oscillations after EAS at the two acupoints in the brain were

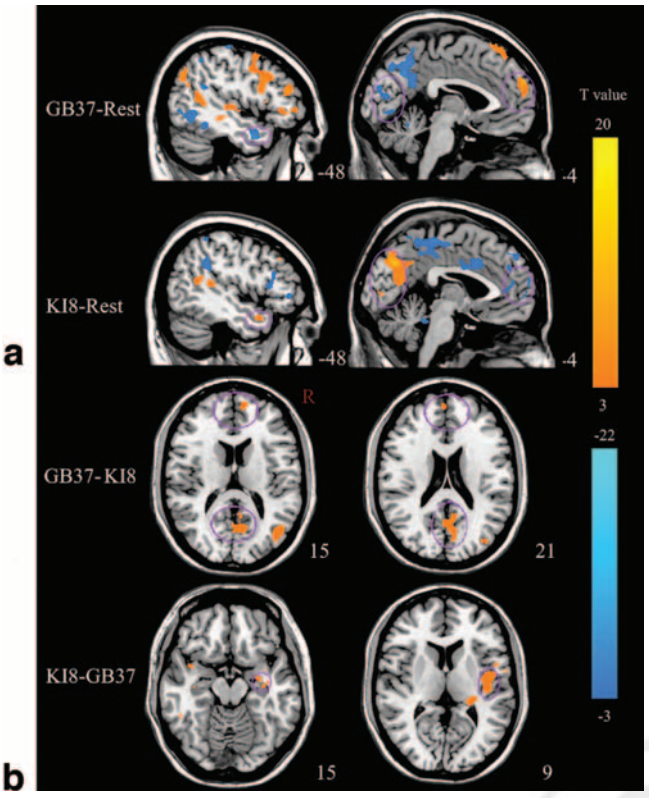

Figure 2. a: Brain regions showing the significantly different patterns of modulating the resting-state functional networks functional networks following EAS (see Table 1). **b:** Brain regions showing the specificity of GB37 and KI8 acupoints (see Table 2) by comparing the functional networks of the two acupoints following EAS.

shown in Figure 1b. Spatial patterns of the brain regions were different after stimulation at the two acupoints. The brain regions at GB37 mainly consisted of the bilateral medial prefrontal cortex (MPFC) (Brodmann area [BA] 10), right dorsolateral prefrontal cortex (DLPFC) (BA 46), supramarginal gyrus, angular cortex, associative visual cortex (BA 19), pC and PCC. The spatial patterns of the brain regions at KI8 mainly consisted of the right MPFC (BA 8/10), bilateral inferior frontal cortex (IFC), bilateral middle frontal cortex (MFC) (BA 11), angular cortex, pC and PCC. The results from the conjunction analysis revealed that the overlapping brain regions were mainly located in the PCC/pC.

Functional Connectivity Results

It was indicated that the functional networks with the overlapping PCC/pC during the resting states (R1) of the two acupoint groups were not significantly different. Results from the paired t-test were shown in Figure 2a and Table 1. After EAS, GB37 and KI8 exerted significant modulation on the resting-state functional networks. However, the visual cortex (BA 17/18/19) at GB37 showed an opposite pattern compared with that of KI8. Such a discrepancy was also present in the MPFC and superior temporal cortex (STC).

Results from the two sample t-test of the two acupoints during the poststimulation state were shown in Figure 2b and Table 2. The most significant and obviously differences were located in the vision-associated regions (BA 18/19), MFC, the right insula, and the right hippocampus.

DISCUSSION

In this study, we used a NRER fMRI design and spatiotemporal approaches to investigate the sustained effects of different acupoints. We reported two findings: (i) It was significantly found that the spatial patterns of the brain regions were distinct. Furthermore, the results of the conjunction analysis showed that the overlapping regions were mainly located in the PCC/pC. (ii)

Table 1
Main Localization of Connectivity Maps by Comparing After Acupuncture Versus Resting at GB37 and KI8 Using a Paired t-Test

Regions	GB37 (Guangming)-Rest						KI8 (Jiaoxin)-Rest				
	Hem	BA	Talairach			t-value	BA	Talairach			T value
			x	y	z			x	y	z	
MFC	L	9/10	−15	28	32	6.14	9/10	−3	55	0	−10.75
	R	9/10	6	56	19	11.21	9/10	3	−18	48	−6.38
STC	L	22	−50	11	−3	−4.22	22	−45	−57	17	6.22
	R						22	56	−57	17	6.99
Occipital cortex (BA17)	L	17	−18	−72	12	−5.86					
	R	17	3	−78	12	−3.88	17	31	−84	4	3.99
Occipital cortex (BA18)	L	18	−12	−80	26	−11.97	18	−3	−80	26	3.65
	R	18	21	−55	3	−6.69	18	12	−90	16	3.81
Occipital cortex (BA19)	L	19	−30	−83	26	−14.32	19	−42	−60	14	6.10
	R	19	12	−86	35	−7.86	19	6	−77	37	5.80
ACC	L										
	R						24/32	9	41	3	−6.92
Insula	L	13	−42	−12	−4	5.53					
	R	13	42	−12	−4	3.58					
Hippocampus	L		−27	−10	−20	5.57					
	R							23	26	−10	−4.06

BA = Brodmann area; Hem = hemisphere; MFC = medial frontal cortex; STC = superior temporal cortex; ACC = anterior cingulate cortex; L = Left; R = right.

Table 2
Main Localization of Specific Effects by Comparing the Poststimulation States Between GB37 and KI8 Using a Two Sample t-Test

Regions	GB37-KI8						KI8-GB37				
	Hem	BA	Talairach			t value	BA	Talairach			t value
			x	y	z			x	y	z	
MFC	L	9/10	−3	53	14	3.86					
	R	9/10	6	42	23	4.04					
PCC/pC	L	31	−3	−51	30	5.59					
	R	31	3	−63	17	4.37					
Occipital cortex	L	18/19	−12	−55	3	3.08					
	R	18/19	42	−67	9	3.66					
Insula	L						13	−42	−15	−4	3.03
	R						13	42	−14	12	3.98
Hippocampus	L							−33	−15	−7	2.88
	R							30	−12	−15	3.40

BA = Brodmann area; Hem = hemisphere; MFC = medial frontal cortex; PCC/pC = posterior cingulate cortex/precuneus; L-Left = R-Right.

We derived the functional connectivity networks from the temporal pattern during the states before and after stimulation associated with the overlapping PCC/pC and detected that the temporal patterns of modulating resting-state functional networks were different between these two acupoints. Furthermore, the functional specificity of the acupoints during the poststimulation state was also demonstrated.

In our study, differential spatial distributions of MPFC, MFC, DLPFC, supramarginal gyrus, angular cortex, MOC, pC, and PCC were found to be associated with the stimulation of GB37 and KI8 (Fig. 1b). These brain regions were also found in the previous acupuncture studies (17–20,29). However, why were the overlapping brain regions mainly located in the PCC/pC following EAS at both GB37 and KI8? Resting-state studies have shown that the metabolism is higher in the cingulate cortex and the spontaneous signal changes are stronger in the PCC/pC (25,30). In disease studies, it has been reported that fMRI signal fluctuations in the PCC/pC is altered in schizophrenia (31). And He et al indicated that the reductions of the low frequent signal fluctuations appear in the pC at the early stages of Alzheimer's disease (32). Recently, another study detected that the PCC/pC plays a pivotal role in the default mode network (33). Of interest, previous acupuncture studies indicated that the PCC/pC is often activated during acupuncture stimulation (18,34,35). Our results implicated that PCC/pC might be an important brain region involved in sustained modulations of acupuncture effects, and these common overlapping regions might reflect the general nonspecific effect of acupoint needling. However, the spatial analysis alone could not provide a clear explanation of the acupuncture effects of these acupoints.

To further investigate the modulation of acupuncture on the DMN, we defined two different brain networks of functional connectivity with the overlapping PCC/pC as a seed region following EAS. We then conducted a paired t-test between the baseline (resting state preceded by any stimulus) and the poststimulation states of different acupoints respectively (Fig. 2a). Although the baselines of the two acupoints were similar, the significant discrepancy was observed in the connectivity changes, which presented an opposite pattern in the vision-related cortex (BA 17/18/19), MPFC and STC at GB37, compared with that at KI8. From the results above, we suggested that different acupoints might exert different influences on the PCC/pC associated with the DMN networks, attributing to the different effects of the acupoints. During a novel and specific task, processing resources are moved from the areas normally engaged in the default mode networks to areas relevant to the presented task. Therefore, we proposed that acupuncture-related effects appearing during the poststimulation state might also induce such resource redistributions.

GB37 is one of the important acupoint used to treat eye diseases, based on TCM. Group analysis between GB37 and KI8 showed that visual cortical regions (BA 18/19) and the MFC were specifically responsive to the stimulation of GB37, suggesting the specificity of GB37 as a vision-specific acupoint. In contrast, the KI8 is generally used to treat menstrual pain, irregular menstruation and gonalgia. The cortical regions might represent the specificity of KI8 in the insula and hippocampus. The insula has an important role in pain intensity coding circuits (36). Although the hippocampus is related to memory and learning processing, it was found that hippocampus may be also involved in the pain-related processing (37). Our findings further supported the view that different effects of acupoints might lead to the resource redistributions because of their different function-guide actions.

CONCLUSION

By applying novel experimental design and analysis methods, this study evaluated the sustained effects of acupuncture related with GB37 and KI8. It was detected that the spatial and temporal patterns of the modulation of acupuncture on the DMN were distinct, which may contribute to the differential functional effects of acupoints. Modulations in the vision-related cortex (BA 18/19) were responsive to the specificity of GB37 as compared with KI8 (a nonvision-related acupoint). However, the specificity of KI8 was associated with pain modulation and the activities in the insula and hippocampus. Our current results also provide neuroimaging data suggesting that a relationship exists

between the specificity of acupuncture treatments and certain disorders.

Additionally, the mechanism underlying acupuncture was complicated and not well-defined. It is essential to use proper approaches to acupuncture studies; hence, our findings reflect a significant methodological contribution combining with both spatial and temporal information.

REFERENCES

1. Diehl DL, Kaplan G, Coulter I, Glik D, Hurwitz EL. Use of acupuncture by American physicians. J Altern Complement Med 1997;3:119–126.
2. Eisenberg DM, Kessler RC, Foster C, Norlock FE, Calkins DR, Delbanco TL. Unconventional medicine in the United States. N Engl J Med 1993;328:246–252.
3. Eisenberg DM, Davis RB, Ettner SL, et al. Trends in alternative medicine use in the United States, 1990-1997 results of a follow-up national survey. Am Med Assoc 1998;280:1569–1575.
4. Acupuncture NIH. NIH consensus development panel on acupuncture. JAMA 1998;280:1518–1524.
5. Siedentopf CM, Golaszewski SM, Mottaghy FM, Ruff CC, Felber S, Schlager A. Functional magnetic resonance imaging detects activation of the visual association cortex during laser acupuncture of the foot in humans. Neurosci Lett 2002;327:53–56.
6. Litscher G, Rachbauer D, Ropele S, et al. Acupuncture using laser needles modulates brain function: first evidence from functional transcranial Doppler sonography and functional magnetic resonance imaging. Laser Med Sci 2004;19:6–11.
7. Li G, Cheung RTF, Ma QY, Yang ES. Visual cortical activations on fMRI upon stimulation of the vision-implicated acupoints. Neuroreport 2003;14:669–673.
8. Parrish TB, Schaeffer A, Catanese M, Rogel MJ. Functional magnetic resonance imaging of real and sham acupuncture. IEEE Eng Med Biol Mag 2005;247:35–40.
9. Knight B, Mudge C, Openshaw S, White A, Hart A. Effect of acupuncture on nausea of pregnancy: a randomized, controlled trial. Obstet Gynecol 2001;97:184–188.
10. Ng DK, Chow P, Ming S, et al. A double-blind, randomized, placebo-controlled trial of acupuncture for the treatment of childhood persistent allergic rhinitis. Pediatrics 2004;114:1242–1247.
11. Li Y, Tougas G, Chiverton SG, Hunt RH. The effect of acupuncture on gastrointestinal function and disorders. Am J Gastroenterol 1992;87:1372–1381.
12. Tsui P, Leung MC. Comparison of the effectiveness between manual acupuncture and electro-acupuncture on patients with tennis elbow. Acupunct Electrother Res 2002;27:107–117.
13. Gareus IK, Lacour M, Schulte AC, Hennig J. Is there a BOLD response of the visual cortex on stimulation of the vision-related acupoint GB 37? J Magn Reson Imaging 2002;15:227–232.
14. Kong J, Kaptchuk TJ, Webb JM, et al. Functional neuroanatomical investigation of vision-related acupuncture point specificity-a multisession fMRI study. Hum Brain Mapp 2009;30:38–46.
15. Cho ZH, Chung SC, Lee HJ, Wong EK, Min BI. Retraction. New findings of the correlation between acupoints and corresponding brain cortices using functional MRI. Proc Natl Acad Sci U S A 2006;103:10527.
16. Cho ZH, Chung SC, Jones JP, et al. New findings of the correlation between acupoints and corresponding brain cortices using functional MRI. Proc Natl Acad Sci U S A 1998;95:2670–2673.
17. Hui KK, Liu J, Makris N, et al. Acupuncture modulates the limbic system and subcortical gray structures of the human brain: evidence from fMRI studies in normal subjects. Hum Brain Mapp 2000;9:13–25.
18. Hui KK, Liu J, Marina O, et al. The integrated response of the human cerebro-cerebellar and limbic systems to acupuncture stimulation at ST36 as evidenced by fMRI. Neuroimage 2005;27:479–496.
19. Napadow V, Makris N, Liu J, Kettner NW, Kwong KK, Hui KK. Effects of electroacupuncture versus manual acupuncture on the human brain as measured by fMRI. Hum Brain Mapp 2005;24:193–205.
20. Yan B, Li K, Xu J, et al. Acupoint-specific fMRI patterns in human brain. Neurosci Lett 2005;383:236–240.
21. Zhang Y, Qin W, Liu P, et al. An fMRI study of acupuncture using independent component analysis. Neurosci Lett 2009;449:6–9.
22. Price DD, Rafii A, Watkins LR, Buckingham B. A psychophysical analysis of acupuncture analgesia. Pain 1984;19:27–42.
23. Dhond RP, Yeh C, Park K, Kettner N, Napadow V. Acupuncture modulates resting state connectivity in default and sensorimotor brain networks. Pain 2008;136:407–418.
24. Qin W, Tian J, Bai L, et al. FMRI connectivity analysis of acupuncture effects on an amygdala-associated brain network. Mol Pain 2008;4:55.
25. Fransson P. Spontaneous low-frequency BOLD signal fluctuations: an fMRI investigation of the resting-state default mode of brain function hypothesis. Hum Brain Mapp 2005;26:15–29.
26. Friston KJ, Frith CD, Liddle PF, Frackowiak RS. Functional connectivity: the principal-component analysis of large (PET) data sets. J Cereb Blood Metab 1993;13:5–14.
27. Hui KK, Nixon EE, Vangel MG, et al. Characterization of the "deqi" response in acupuncture. BMC Complement Altern Med 2007;7:33–49.
28. Fox MD, Snyder AZ, Vincent JL, Corbetta M, Van Essen DC, Raichle ME. The human brain is intrinsically organized into dynamic, anticorrelated functional networks. Proc Natl Acad Sci U S A 2005;102:9673–9678.
29. Li G, Liu HL, Cheung RT, et al. An fMRI study comparing brain activation between word generation and electrical stimulation of language-implicated acupoints. Hum Brain Mapp 2003;18:233–238.
30. Raichle ME, MacLeod AM, Snyder AZ, Powers WJ, Gusnard DA, Shulman GL. A default mode of brain function. Proc Natl Acad Sci U S A 2001;98:676–682.
31. Bluhm RL, Miller J, Lanius RA, et al. Spontaneous low-frequency fluctuations in the BOLD signal in schizophrenic patients: anomalies in the default network. Schizophr Bull 2007;33:1004–1012.
32. He Y, Wang L, Zang Y, et al. Regional coherence changes in the early stages of Alzheimer's disease: a combined structural and resting-state functional MRI study. Neuroimage 2007;35:488–500.
33. Fransson P, Marrelec G. The precuneus/posterior cingulate cortex plays a pivotal role in the default mode network: evidence from a partial correlation network analysis. Neuroimage 2008;42:1178–1184.
34. Kong J, Ma L, Gollub RL, et al. A pilot study of functional magnetic resonance imaging of the brain during manual and electroacupuncture stimulation of acupuncture point (LI-4 Hegu) in normal subjects reveals differential brain activation between methods. J Altern Complement Med 2002;8:411–419.
35. Fang J, Jin Z, Wang Y, et al. The salient characteristics of the central effects of acupuncture needling: limbic-paralimbic-neocortical network modulation. Hum Brain Mapp 2009;30:1196–1206.
36. Brooks JC, Tracey I. The insula: a multidimensional integration site for pain. Pain 2007;128:1–2.
37. Dutar P, Lamour Y, Jobert A. Activation of identified septo-hippocampal neurons by noxious peripheral stimulation. Brain Res 1985;328:15–21.